Nuclear Instruments and Methods in Physics Research B 326 (2014) 185–189

Contents lists available at ScienceDirect

Nuclear Instruments and Methods in Physics Research B

journal homepage: www.elsevier.com/locate/nimb

Molecular dynamics computer simulations of sputtering of benzene sample by large mixed Lennard-Jones clusters

L. Rzeznik [a,*], Z. Postawa [b]

[a] University of Information Technology and Management, Sucharskiego 2, 35-225 Rzeszów, Poland
[b] Institute of Physics, Jagiellonian University, Reymonta 4, 30-059 Kraków, Poland

ARTICLE INFO

Article history:
Received 1 July 2013
Received in revised form 15 October 2013
Accepted 22 October 2013
Available online 24 January 2014

Keywords:
Computer simulations
Sputtering
Large noble gas projectiles
SIMS
Organic solids

ABSTRACT

Molecular dynamics computer simulations have been used to probe the role of the projectile composition on the emission efficiency and the sample damage. A benzene crystal was bombarded by 15 keV large heterogeneous noble gas clusters containing 2953 atoms. The projectiles used in this study are two-component clusters composed of Ne, Ar, and Kr atoms directed at 0° and 60° relative to the surface normal. It has been found that for normal incidence the total sputtering yield decreases with the projectile mass, whereas for 60° impact angle the yield increases with this quantity. For both 0° and 60° impact angles the observed sputtering yield for heterogeneous clusters cannot be calculated as a sum of sputtering yields obtained for homogeneous projectiles multiplied by the concentration of each component in the multi-component cluster. The difference in deposition scenarios of the primary kinetic energy is shown to be responsible for the observed behavior of the total sputtering yield.

1. Introduction

The process of surface erosion stimulated by impacts of energetic particles which leads to removal of surface atoms to vacuum, is called sputtering. One of the most important factors characterizing sputtering process is the sputtering yield. This quantity is defined as the amount of material removed from the target surface by an impact of a single projectile. The dependence of the sputtering yield on the beam as well as the target properties has been an object of investigations since the sputtering was first discovered more than 150 years ago. The progress in collecting experimental data has been followed by a development of theoretical models of sputtering [1]. The main focus of all these studies was to predict ejection characteristics of particles emitted from solid surfaces by single component projectiles (atomic and clusters).

The sputtering process has been utilized in numerous technological applications and analytical techniques. One of the most successful analytical techniques that utilize sputtering is so called Secondary Ion Mass Spectrometry (SIMS) [2]. Nowadays SIMS is a well-established tool for chemical characterization of materials. One of the most promising applications of SIMS is 3D imaging of organic systems. Monoatomic keV projectiles are found not to be very useful in such analysis as they usually lead to a significant morphology buildup and damage accumulation [3]. The situation has improved when atomic projectiles were replaced by cluster projectiles [4]. Large Ar clusters with a few hundred atoms were found to be especially useful as they can significantly reduce both the morphology buildup and the damage accumulation, and stimulate ejection of almost unfragmented molecules. The most important deficiency of these clusters is a relatively low ionization efficiency of ejected species caused by a low kinetic energy per atom and by an inert character of atoms composing these projectiles [5]. As a result, it has been suggested that multi-component cluster projectiles, particularly containing hydrogen, could be a better choice. Experiments using a coronene cluster beam were inconclusive, despite the increase of the ion yield due to the extra hydrogen in the beam. However, it must be noted that these experiments were performed with a very low projectile dose [6]. There are also experiments using extremely large and highly charged water clusters where very high molecular ion yields were observed [5,7].

A rapid progress in experimental studies of large clusters sputtering of organic solids is, however, not accompanied by an adequate progress in theoretical understanding of the sputtering process initiated by such massive projectiles. For instance, there are no studies of sputtering process initiated by multi-component large projectiles. In the current research molecular dynamics computer simulations are employed to investigate the emission efficiency from a benzene sample caused by an impact of 15 keV multi-component large noble gas cluster projectiles. The projectiles used in this study were two-component clusters composed of Ne, Ar, and Kr atoms. The results obtained for such heterogeneous projectiles are compared to the data obtained for

* Corresponding author.
E-mail address: rzeznik@lippmann.lu (L. Rzeznik).

0168-583X/$ - see front matter © 2014 Elsevier B.V. All rights reserved.
http://dx.doi.org/10.1016/j.nimb.2013.10.060

single-component Ne, Ar, and Kr clusters [8]. The main question addressed in the current study is, whether, and to what extent, it is possible to estimate the sputtering yield for heterogeneous projectiles from the data obtained for single-component clusters. In particular, we would like to check if the total sputtering yield will depend on the relative concentration of atoms in heterogeneous projectiles.

2. Model

Details of the MD computer simulations used to model cluster bombardment are described elsewhere [9]. The interactions between Ne, Ar, and Kr atoms in the projectile and between the projectile atoms and all other particles in the system are described by the Lennard-Jones potential splined with the KrC potential to properly describe high-energy collisions [10]. In this study we used the following form of the Lennard-Jones potential, $V_{ij} = \varepsilon_{ij}[(\sigma_{ij}/r_{ij})^{12} - 2(\sigma_{ij}/r_{ij})^{6}]$, where the parameter ε denotes the well depth and σ depicts the equilibrium distance. The values of the Lennard-Jones potential parameters ε_{ij} and σ_{ij} describing the interaction between the same type of atoms were set to: ε_{Ne-Ne} = 3 meV, σ_{Ne-Ne} = 3.13 Å [11], ε_{Ar-Ar} = 10.3 meV, σ_{Ar-Ar} = 3.82 Å, ε_{Kr-Kr} = 14.4 meV, σ_{Kr-Kr} = 4.0779 Å [12], whereas for different atom types they were calculated using Lorentz-Berthelot mixing rules: $\varepsilon_{ij} = (\varepsilon_{ii}\varepsilon_{jj})^{1/2}$, $\sigma_{ij} = 0.5 \cdot (\sigma_{ii} + \sigma_{jj})$. The model approximating the benzene crystal consists of 307366 molecules arranged in a hemispherical sample of the radius 26 nm. A coarse-grained approximation is used to model the benzene solid, in which each benzene molecule is represented by six CH particles with the mass of 13 amu. This approach allows decreasing significantly the time of simulations while giving sputtering results similar to the data obtained with a full atomistic model [13]. The CH–CH interaction inside a single benzene molecule is described by a Morse potential. The Lennard-Jones potential is used to describe the interaction of CH–CH particles located in different molecules. Details of the coarse-grained method and the appropriate values for the Lennard-Jones and Morse potential parameters can be found elsewhere [13]. All projectiles used in this study have the kinetic energy of 15 keV and the size of 2953 atoms, which gives the energy per atom of approximately 5 eV. Each heterogeneous projectile is a two-component cluster in which the concentration of a certain atom type was set to 0%, 25%, 50%, 75%, and 100%. For multi-component projectiles the velocity of atoms was set to preserve the total kinetic energy of the projectile. The radius of the clusters varies from 2.5 nm for pure Ne_{2953} to 3.1 nm for pure Kr_{2953}. It is known that such a small change in the projectile size does not affect the sputtering efficiency [14].

3. Results and discussion

The dependence of the total sputtering yield on the projectile mass for impact angles 0° and 60° is shown in Fig. 1. Several observations can be derived from this figure. Firstly, the sputtering yield is influenced by both the projectile mass and the angle of incidence. The dependence on the mass is monotonic, i.e. data points corresponding to heterogeneous clusters preserve a general trend observed for single-component projectiles. The total sputtering yield decreases with the projectile mass for normal incidence, whereas the opposite trend is visible for 60° impact angle. In general, changing the impact angle from 0° to 60° makes the emission from the sample more efficient, although a degree of this enhancement is different for different cluster projectiles. For the lightest Ne_{2953} projectile only a slight increase of the yield is visible. In this case, the enhancement factor is barely 1.1, whereas for the heaviest Kr_{2953} this effect is very pronounced. The sputtering yield for 60° impact angle of this cluster is nearly 40 times larger than for the normal impact.

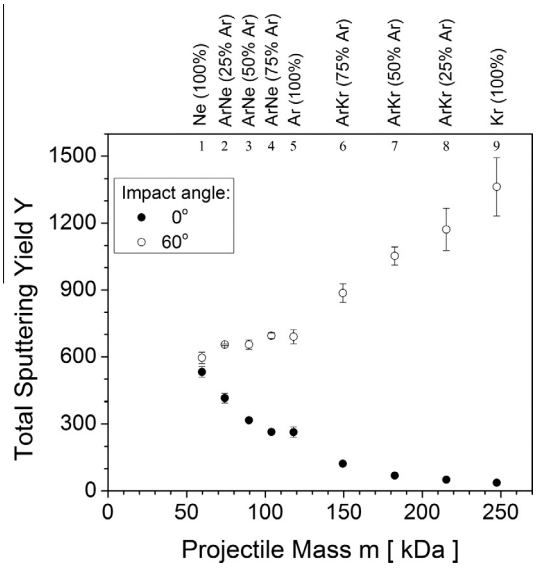

Fig. 1. The total sputtering yield dependence on the projectile mass for two impact angles 0° and 60° for 15 keV single- and two-component cluster projectiles composed of 2953 noble gas atoms (Ne, Ar, and Kr). The labels at the upper part of the Figure indicate the projectiles used in the study.

The yield enhancement for 60° impact angle compared to the normal incidence has already been observed for large clusters composed of Ar atoms by both theoretical studies [8,15–17] and the experiment [18]. Although similar behavior was reported in the studies performed with atomic projectiles [19], the physics of the processes leading to the signal increase in these two cases is different. For atomic bombardment the total sputtering yield is a result of the interplay between the depth of the primary energy deposition and the amount of energy backreflected from the surface. The influence of these two processes on the emission efficiency is opposite with the increase of the impact angle. The sputtering yield benefits from the shift of the energy deposition profile closer to the surface when the angle of incidence increases. However, at the same time the yield becomes smaller as the total amount of deposited energy is reduced due to a more efficient backreflection of the primary energy when the impact angle becomes more oblique. As a result, the total sputtering yield has a maximum at the impact angle around 50–70°.

For cluster projectile the depth of primary energy deposition is also important. However, as the primary energy is usually deposited closer to the surface as compared to the impact of atomic projectiles with the same kinetic energy, the effect of this process is less critical. There are, however, two new phenomena that are also important. Large projectiles are composed of large number of atoms. After impact along directions close to the surface normal a dense cloud of projectile atoms penetrating downward the sample plays a role of a blocker that prevents the emission of molecules located below the projectile [8,15–17]. On the other hand, such cloud does not form when the projectile is directed at oblique impact angles as the projectiles atoms are quickly backreflected into the vacuum. As a result, at these impact angles the blocking effect will be minimized. In fact, reduction of the blocking effect is not the only process that will enhance molecular ejection as a dense flux of backreflected projectile atoms will entrain sample molecules when sliding over the rim of the crater. As a result, additional molecules will be "washed out" from the organic material and the sputtering yield will increase. The effectiveness of the last two processes increases with the number of atoms in the projectile

which are involved in either "blocking" or "washing out" effects. As a result, these phenomena are not observed for smaller projectiles [15].

As shown in Fig. 1, the sputtering yield for both 0° and 60° impact angles depends also on the mass of the projectile. Once more, several phenomena should be invoked to explain this observation. First factor will be again the depth of energy deposition. Popok et al. have observed that for cluster projectiles the projectile range depends in a linear way on the projectile momentum [20]. The dependence of the penetration depth of the cluster projectiles used in this study on their momentum is presented in Fig. 2. The penetration range was calculated as the average over the maximum penetration depth of each constituent projectile atom. It can be seen that the projectile momentum indeed influences the projectile range. The range scales linearly with the momentum, although the slope of this curve is slightly different for clusters containing Ar–Ne and Ar–Kr atoms and is also dependent on the angle of incidence. Not surprisingly, the range is much larger for normal incidence. For 0° impact angle the lightest Ne_{2953} cluster, having the lowest momentum, penetrates, on average, over 5 nm through the sample, whereas the Kr_{2953} projectile, having the momentum twice larger than Ne_{2953}, penetrates through the target to the depth of around 9.5 nm, which roughly agrees with predictions of Popok et al. As a consequence, the Kr_{2953} projectile will deposit its energy much deeper than the Ne_{2953} cluster. Moreover, Kr_{2953} does not only penetrate deeper but has also lower velocity as compared to lighter projectiles, which is indicated as v_X at the upper part of the figure. Having both lower velocity and higher penetration depth the Kr_{2953} cluster needs more time to share its energy with the target molecules. With the assumption adopted from the work of Garrison et al. that the process of energy deposition ends when the 90% of the projectile energy is deposited [21], the calculated energy deposition time for the Kr_{2953} is 5.2 ps, whereas most of the primary kinetic energy is already deposited at 1.5 ps for the Ne_{2953} projectile. As a result, the duration of the blocking effect during Kr_{2953} impact is expanded in time. There is also more time for the deposited energy to be carried away from the region from where the ejection occurs [6], and, consequently, much lower emission of the substrate particles is observed.

The opposite situation occurs for the impact angle of 60°. The observed discrepancies in the average penetration depth between

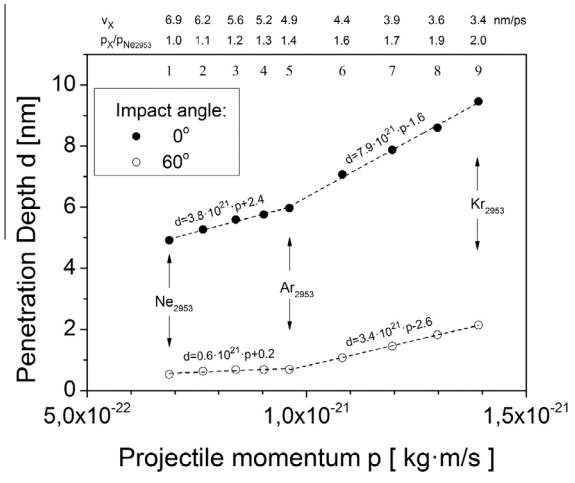

Fig. 2. Dependence of the projectile penetration depth, d, on the projectile momentum, p. Numbers 1–9 indicate given projectiles as defined in Fig. 1. Pure Ne_{2953}, Ar_{2953}, and Kr_{2953} clusters are additionally indicated by arrows. The energy of each projectile is 15 keV. Projectile momentum, p_X, normalized to the momentum of a pure Ne_{2953} projectile as well as the velocities of the clusters, v_X, are shown at the upper part of the plot. Dashed lines denote the linear regression fits of a formula $d = a * p + b$.

all projectiles are only around 1.5 nm. For this impact angle the projectiles travel through the sample rather horizontally. As most of the projectile primary kinetic energy is deposited in the volume that can contribute to ejection, larger length of the penetration path along the surface will result in a stronger emission. As a result, the Kr_{2953} cluster having the highest momentum and, consequently, the longest penetration path along the sample surface will lead to emission of the largest number of molecules as indeed indicated in Fig. 1. At very large impact angles the primary energy backreflection cannot be neglected. The effectiveness of this process increases with a decrease of the projectile mass [8], which additionally will enhance the effectiveness of the emission process for projectiles composed of heavy atoms.

The data presented in Fig. 1 have been plotted as a function of the projectile mass. This allows comparing the data obtained for projectiles having the same energy and size. However, the clarity of such plot will be blurred after adding points coming from projectiles having a different size or primary kinetic energy. It has been observed, however, that this dependence can be greatly simplified if the sputtering yield per single nucleon of the projectile is expressed as a function of the projectile kinetic energy per nucleon, ε [6,22]. In general, several regions can be identified in such plot. In each region the character of the sputtering process is different. In the region located below 1 eV/nucleon the soft desorption occurs [6]. In this energy range the sputtering yield per nucleon decreases nonlinearly with a decrease of ε and the fragmentation process is significantly reduced [6]. In the second region, which extends from 1 eV/nucleon up to around 100 eV/nucleon the projectile energy is high enough to cause fragmentation of sample molecules. In this region the linear dependence of the total sputtering yield per nucleon on the projectile energy ε is observed [6]. However, when the ε becomes too large, the projectile begins to deposits its energy too deep inside the bombarded material and the yield starts to diminish [23].

Circles in Fig. 3 present the data from Fig. 1 replotted in the form discussed above. It is evident that for the conditions used in this study all data points belong to the region of soft sputtering, where no fragmentation is observed. For normal incidence the total sputtering yield per nucleon decreases with a decrease of the ε and a sharp change in the curve inclination when going from the ArNe to the ArKr clusters is observed. The slope of the curve plotted for 60° impact angle is much smaller than for normal incidence and the curve has a similar slope for all investigated values of ε. The yield per nucleon is only weekly dependent on ε. The yields of single-component projectiles are indicated by arrows. It is evident that the yield stimulated by the impact of multi-component projectiles is located between the yields resulted from the impacts of single-component clusters. It would be interesting, therefore, to determine if the sputtering yield for a heterogeneous projectile $Y(A_nB_m)$, $n + m = 2953$, could be estimated from the yields obtained for pure clusters, $Y(A_{2953})$ and $Y(B_{2953})$, and from the concentration of given elements in the two-component cluster, c_A and c_B. Adopting formula used to calculate partial sputtering yields from two-component alloys [24], the total sputtering yield induced by an impact of a heterogeneous cluster can be expressed as:

$$Y(A_nB_m) = c_A Y(A_{n+m}) + c_B Y(B_{n+m}), \quad (1)$$

where $c_A = n/2953$, $c_B = m/2953$, n and m are the number of atoms of type A and B in the two-component projectile, respectively.

Crosses in Fig. 3 indicate the estimated values of the sputtering yields obtained from the Eq. (1), while closed and empty circles depict the data obtained by the MD simulations. For 0° impact angle, apart from the data points 1, 5, and 9 which indicate single-component Ne, Ar, and Kr clusters, the agreement is poor. In this case all predicted data points are located above the values obtained from the MD simulations. This means that the multi-component

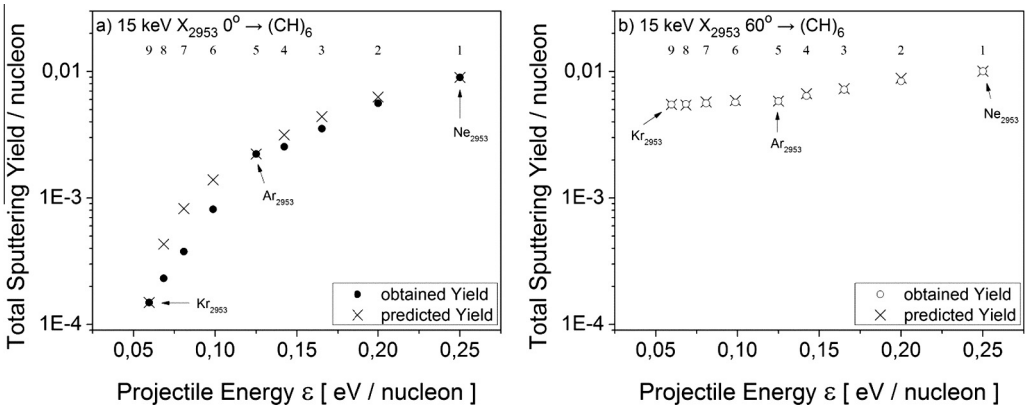

Fig. 3. Dependence of the total sputtering yield per nucleon on the projectile energy per nucleon for (a) 0° and (b) 60° impact angles. The X_{2953} symbol depicts single- and two-component clusters composed of 2953 noble gas atoms (Ne, Ar, and Kr). Closed and open circles indicate the results of the MD simulations, whereas crosses represent the predictions given by Eq. (1).

projectiles remove material less efficiently than their single-component counterparts. In contrast, the agreement observed for 60° impact angle is good. However, it may be caused mainly by the fact that at this impact angle the yields obtained for single-component Ne, Ar, and Kr projectiles are very similar. Therefore, even erroneous formula will not have a visible effect on the final results. We conclude, therefore, that the Eq. (1) cannot be used to predict sputtering yields induced by an impact of multi-component projectiles.

As it was already indicated, the emission efficiency depends on the average penetration depth of the projectile atoms. That is why for two-component projectiles the penetration depth should be also considered separately for both types of atoms composing such clusters. Fig. 4 shows, one more time, the dependence of the average penetration depth on the projectile energy per nucleon. However, this time, the penetration depth is separated into two parts. Each part is related to the appropriate type of atoms composing the multi-component cluster. The horizontal lines present the depths achieved with single-component Ne, Ar, and Kr clusters. It is evident that for multi-component cluster composed of Kr and Ar atoms the average penetration depths reached by its constituents do not match with the values obtained for the entire cluster. In fact, the data indicate that the average depth is larger for Ar and smaller for Kr when compared to the depths reached by single-component projectiles. Such behavior can be attributed to the "clearing the way" effect, in which atoms composing the heavier component of a heterogeneous cluster penetrate deeper and clear the way for the lighter component. As a result, the penetration depth of the lighter atoms increases, which decreases their ability to stimulate sputtering at normal incidence. At the same time the range of the heavier atoms is reduced due to a smaller number of these atoms in the projectile, which should increase the contribution to the yield stimulated by this group of atoms.

Our results indicate, therefore, that when the concentration of a particular atom type in a multi-component projectile is changing, the average depth of penetration of such group of atoms varies rather with the mass of the resulting cluster than with the concentration of this group of atoms. As a result, the atom concentration in a multi-component projectile is not the only factor which determines the yield change between the values characteristic for 0% and 100% concentration. The "clearing the way" effect is an additional factor that should be taken into account for these projectiles.

The "clearing the way" effect is more important for these two-component projectiles for which the ranges achieved by their one-component equivalents differ significantly. For 0° impact angle the range of a pure Kr projectile is around 3.5 nm larger than for a pure Ar cluster. As a result, Ar atoms in a mixed ArKr projectile can follow Kr atoms to a larger depth than it takes place for 60° impact angle, where the ranges of pure Kr and Ar clusters differ by only 1 nm. For ArNe clusters for both investigated impact angles the "clearing the way" effect is statistically invisible as ranges of pure Ar and Ne clusters are quite similar.

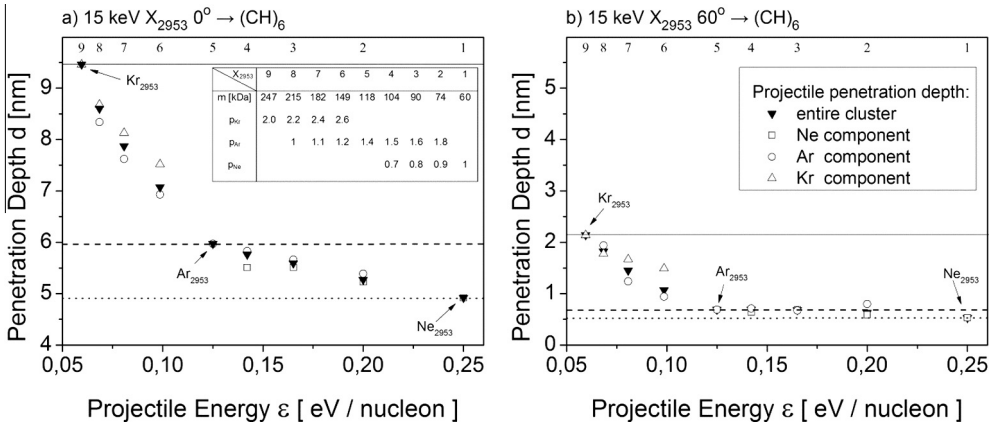

Fig. 4. The projectile penetration depth as a function of the projectile kinetic energy per nucleon for (a) 0° and (b) 60° impact angles. Closed triangles denote the average penetration depth of the entire projectile, while open symbols indicate penetration depths of a given type of atoms: Ne (squares), Ar (circles), and Kr (triangles). Solid, dashed, and dotted lines represent penetration depths of pure Kr_{2953}, Ar_{2953}, and Ne_{2953} cluster projectiles, respectively.

There is one more interesting observation that can be derived from Fig. 4 if not only a penetration depth but also the projectile momentum is calculated separately for both types of atoms composing a multi-component cluster. The momentum calculated individually for each type of atoms composing the heterogeneous cluster normalized to the momentum of a single Ne atom in the pure Ne_{2953} projectile is presented as p_{Kr}, p_{Ar}, and p_{Ne} in the rows 3–5 of the inset to Fig. 4a. It is evident that, when the mass of the projectile, m, is decreasing, the momentum of both the heavier as well as the lighter component increases and vice versa. However, when comparing the momentum of each constituent atom in a heterogeneous projectile to its homogeneous equivalents it can be seen that the momentum of the heavier atoms increases, whereas the momentum of the lighter atoms decreases in such a multi-component cluster. As a result, in such projectile heavier atoms should penetrate deeper inside the sample and the penetration depth of lighter atoms should be reduced. Surprisingly, a completely opposite trend is observed in our data. The lighter atoms of the heterogeneous cluster penetrate deeper while the heavier atoms have a smaller range as compared to their counterparts in pure clusters. We can again attribute this observation to the "clearing the way" effect, in which lighter atoms, despite having lower momentum as compared to atoms in a homogeneous cluster, can penetrate deeper just by following the heavier atoms.

4. Conclusions

We have investigated the effect of the projectile composition and the impact angle on the sputtering process of organic molecules emitted from the benzene crystal bombarded by 15 keV large two-component cluster projectiles composed of Ne, Ar, and Kr atoms. It has been shown that both the projectile mass and the impact angle influence the sputtering yield. For normal incidence the emission efficiency decreases with the projectile mass whereas an opposite trend is observed for 60° impact angle. The dependence of the sputtering yield on the projectile mass for a two-component cluster cannot be described by the sum of the yields calculated for homogeneous projectiles multiplied by the concentration of each component in a heterogeneous cluster. It is also shown that the different components of a heterogeneous cluster penetrate to different depths and these depths change when the composition of such cluster changes.

Acknowledgments

The financial support from the National Science Centre program no 2011/01/D/ST4/05070 is gratefully acknowledged. This research was supported in part by PL-Grid Infrastructure.

References

[1] P. Sigmund, Phys. Rev. 184 (1969) 383.
[2] A. Benninghoven, Z. Phys. A Atoms Nucl. 220 (1969) 159.
[3] N. Winograd, Surf. Interface Anal. 45 (2013) 3.
[4] S. Ninomiya, Y. Nakata, K. Ichiki, T. Seki, T. Aoki, J. Matsuo, Nucl. Instr. Meth. Phys. Res. B 256 (2007) 493.
[5] S. Sheraz, A. Barber, J.S. Fletcher, N.P. Lockyer, J.C. Vickerman, Anal. Chem. 85 (2013) 5654.
[6] A. Delcorte, B.J. Garrison, K. Hamraoui, Anal. Chem. 81 (2009) 6676.
[7] D. Asakawa, K. Hiraoka, Rapid Commun. Mass Spectrom. 25 (2011) 655.
[8] L. Rzeznik, R. Paruch, B.J. Garrison, Z. Postawa, Acta Phys. Pol. A 123 (2013) 825.
[9] B.J. Garrison, Z. Postawa, Mass Spectrom. Rev. 27 (2008) 289.
[10] R.A. Aziz, M.J. Slaman, Mol. Phys. 58 (1986) 679.
[11] C.P. Herrero, Phys. Rev. B 68 (2003) 172104.
[12] S.H. Min, C.M. Son, S.H. Lee, Bull. Korean Chem. Soc. 28 (2007) 1689.
[13] E.J. Smiley, Z. Postawa, I.A. Wojciechowski, N. Winograd, B.J. Garrison, Appl. Surf. Sci. 252 (2006) 6436.
[14] T. Aoki, T. Seki, J. Matsuo, Nucl. Instr. Meth. Phys. Res. B 267 (2009) 2999.
[15] B. Czerwinski, L. Rzeznik, R. Paruch, B.J. Garrison, Z. Postawa, Nucl. Instr. Meth. Phys. Res. B 269 (2011) 1578.
[16] Z. Postawa, R. Paruch, L. Rzeznik, B.J. Garrison, Surf. Interface Anal. 45 (2013) 35.
[17] L. Rzeznik, R. Paruch, B.J. Garrison, Z. Postawa, Surf. Interface Anal. 45 (2013) 27.
[18] D. Rading, R. Möllers, H.G. Cramer, F. Kollmer, W. Paul, E. Niehuis, Surf. Interface Anal. 45 (2013) 171.
[19] R. Behrisch, W. Eckstein, Sputtering by Particle Bombardment: Experiments and Computer Calculations from Threshold to MeV Energies, Springer, Berlin, 2007 and references therein.
[20] V.N. Popok, J. Samela, K. Nordlund, E.E.B. Campbell, Phys. Rev. B 82 (2010) 201403(R).
[21] K.E. Ryan, E.J. Smiley, N. Winograd, B.J. Garrison, Appl. Surf. Sci. 255 (2008) 844.
[22] C. Anders, H.M. Urbassek, R.E. Johnson, Phys. Rev. B 70 (2004) 155404.
[23] G. Palka, L. Rzeznik, R. Paruch, Z. Postawa, Acta Phys. Pol. A 123 (2013) 831.
[24] R. Behrisch, W. Eckstein (Eds.), Sputtering by Particle Bombardment: Experiments and Computer Calculations from Threshold to meV Energies, Topics Appl. Physics 110, Springer-Verlag BERLIN, Germany, 2007, and references therein.